



# Transport of Atom Packets in a Train of Ioffe-Pritchard Traps

Thierry Lahaye, Gael Reinaudi, Zhaoying Wang, Antoine Couvert, David Guéry-Odelin

► **To cite this version:**

Thierry Lahaye, Gael Reinaudi, Zhaoying Wang, Antoine Couvert, David Guéry-Odelin. Transport of Atom Packets in a Train of Ioffe-Pritchard Traps. 2006. <hal-00068349>

**HAL Id: hal-00068349**

**<https://hal.archives-ouvertes.fr/hal-00068349>**

Submitted on 11 May 2006

**HAL** is a multi-disciplinary open access archive for the deposit and dissemination of scientific research documents, whether they are published or not. The documents may come from teaching and research institutions in France or abroad, or from public or private research centers.

L'archive ouverte pluridisciplinaire **HAL**, est destinée au dépôt et à la diffusion de documents scientifiques de niveau recherche, publiés ou non, émanant des établissements d'enseignement et de recherche français ou étrangers, des laboratoires publics ou privés.

# Transport of Atom Packets in a Train of Ioffe-Pritchard Traps

T. Lahaye, G. Reinaudi, Z. Wang, A. Couvert and D. Guéry-Odelin  
*Laboratoire Kastler Brossel\*, 24 rue Lhomond, F-75231 Paris Cedex 05, France*

(Dated: May 11, 2006)

We demonstrate transport and evaporative cooling of several atomic clouds in a chain of magnetic Ioffe-Pritchard traps moving at a low speed ( $< 1$  m/s). The trapping scheme relies on the use of a magnetic guide for transverse confinement and of magnets fixed on a conveyor belt for longitudinal trapping. This experiment introduces a new approach for parallelizing the production of Bose-Einstein condensates as well as for the realization of a continuous atom laser.

PACS numbers: 32.80.Pj, 03.75.Pp

The combination of laser cooling and evaporative cooling has led in the last decade to a revolution in atomic physics, with the achievement of Bose-Einstein Condensation (BEC) in alkali vapors [1]. This breakthrough was followed by many spectacular experiments, among which the realization of coherent atom sources [2] that are the equivalent of a laser for matter waves. However the available mean flux of quantum-degenerate atoms has remained limited to values between  $10^4$  and  $10^6$  per second. Larger fluxes would be highly beneficial for applications such as lithography or interferometry.

A natural way to increase the production rate of Bose-Einstein condensates is to increase the duty cycle of laser cooling in the magneto-optical trap (MOT), which is extremely efficient in terms of cooling rate. For that purpose, one needs to operate the various steps of evaporative cooling *at the same time*, at a location differing from the one where laser cooling takes place. A first possibility, proposed in [3] and preliminarily demonstrated in [4], lies in the production, by means of laser cooling techniques, of a magnetically guided atomic beam on which evaporative cooling can then be applied spatially. In this case the duty cycle of laser cooling is typically 50%. Another option consists in transferring a cloud of cold atoms in a three-dimensional magnetic trap and then move it away from the MOT, in order to load the latter again. The trapped cloud can then be evaporated ‘on the fly’ in this moving trap, provided no heating and no spin-flip losses occur.

Magnetic transport has already been demonstrated in macroscopic traps moving mechanically [5] or using a set of coils with time-varying currents [6]. Those traps use a three-dimensional quadrupole configuration with a vanishing field at the center, which prevents evaporation to degeneracy. On atom chips, the transport of ultracold [7] and even of Bose-condensed clouds [8] has been demonstrated, but still with limited fluxes.

In this Letter, we demonstrate transport and evaporative cooling of several atom clouds in a chain of moving Ioffe-Pritchard traps. The transverse confinement is ensured by a magnetic guide creating a two-dimensional quadrupole field, and a spatially varying longitudinal field created by permanent magnets fixed on a conveyor

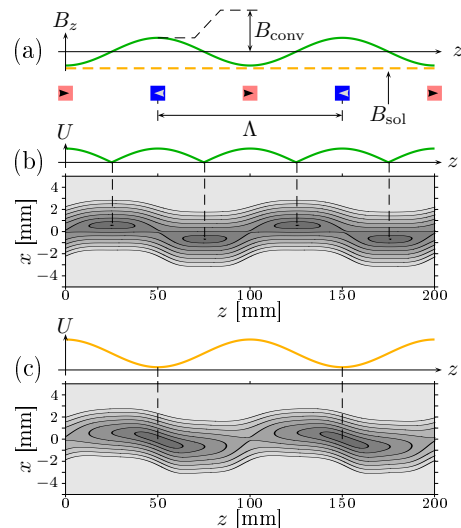


FIG. 1: (Color online). Creation of a longitudinal confinement with permanent magnets. (a): Magnets with alternating magnetization directions (arrows) located on a line parallel to  $z$  create a modulated  $z$ -component of the magnetic field (solid line). A constant offset field  $B_{sol}$  (dashed line) can be added in order to keep a constant sign for  $B_z$ . (b): The potential  $U$  experienced by the atoms for  $B_{sol} = 0$  is a chain of quadrupole traps (top curve). Due to the transverse component  $B_x$  of the field, the traps are shifted from the guide axis, as can be seen on the contour plot of  $|\mathbf{B}|$  in the  $(xz)$  plane. The iso-contours are plotted every 20 G, starting at 0 G. (c): With a large enough  $B_{sol}$ , one gets a chain of on-axis Ioffe-Pritchard traps.

belt provides a moving longitudinal trapping. We show that this setup can be used to transport an atom cloud at a speed as low as 25 cm/s, without any detectable heating, and that we can simultaneously transport and cool several clouds, each containing about  $10^9$  atoms.

The setup used to produce a magnetically guided atomic beam of  $^{87}\text{Rb}$  in the collisional regime has been described elsewhere [9]. Packets containing  $2 \times 10^9$  atoms in the  $|F = -m_F = 1\rangle$  state are injected every 200 ms into a 4.5 m long magnetic guide generating a transverse gradient  $b = 800$  G/cm. Due to their longitudinal velocity dispersion, they spread and overlap, resulting in a continuous beam after typically 50 cm of propagation.

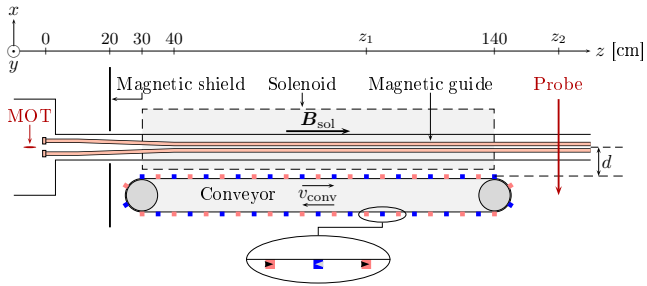


FIG. 2: (Color online). Experimental setup.

A train of magnetic traps is obtained by superimposing a corrugated bias field  $B_z$  along the guide axis, which creates longitudinal potential barriers. This is achieved with permanent magnets located on a line parallel to the guide axis. In practice, they are separated by a distance  $\Lambda/2 = 5$  cm (see Fig. 1a). The resulting potential consists in a chain of three-dimensional quadrupole traps (Fig. 1b). By adding with a solenoid a uniform longitudinal field  $B_{\text{sol}}$  higher than the corrugation amplitude  $B_{\text{conv}}$ , two successive quadrupole traps merge into a single Ioffe-Pritchard (IP) trap (Fig. 1c). For a given configuration, the IP trap depth is twice the one of a quadrupole trap.

In order to let the resulting traps move along  $z$  at a controllable velocity  $v_{\text{conv}}$ , the magnets are fixed on a conveyor belt. The practical arrangement is shown schematically on Fig. 2. The conveyor belt supporting 50 magnets is parallel to the guide axis, at an adjustable distance  $d$ . This allows us to vary the height of the magnetic field barriers experienced by the atoms, since the corrugation amplitude  $B_{\text{conv}}$  scales approximately as  $\exp(-2\pi d/\Lambda)$  [10]. We use  $20 \times 10 \times 10$  mm<sup>3</sup> rare-earth (Nd-Fe-B) permanent magnets [11] with a magnetization of about 800 kA/m, yielding a field amplitude  $B_{\text{conv}} \simeq 25$  G for a distance  $d \simeq 45$  mm. The resulting IP traps have a depth of  $2B_{\text{conv}} = 50$  G, a typical offset field  $B_{\text{sol}} - B_{\text{conv}} \simeq 1$  G, a transverse gradient  $b \simeq 800$  G/cm, and a longitudinal curvature on the order of  $10$  G/cm<sup>2</sup>. The corresponding axial and transverse frequencies are 3 and 720 Hz, respectively. The barrier height increases fast at the entrance of the conveyor (for  $z < 30$  cm), which permits an efficient capture of atom clouds launched into the guide.

The conveyor is set in motion by an electric motor and its speed  $v_{\text{conv}}$  can be adjusted between 10 and 130 cm/s. The measured speed fluctuations are below 2%. The depths of successive wells vary by as much as 5% due to the dispersion in the magnetization of the magnets. However, by contrast to magnetic transport systems using time-varying currents in a set of coils, the geometry of a given trap, in the moving frame, is constant by construction, even far from the trap minimum. This prevents any strong heating due to the deformations of the trap

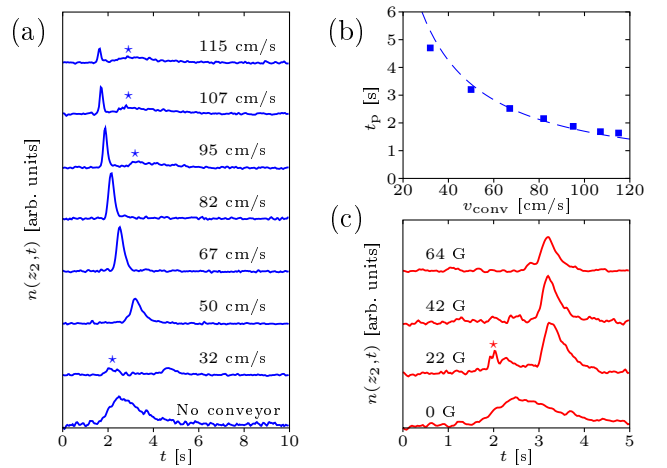


FIG. 3: (Color online). Absorption of a probe beam located at  $z_2 = 1.7$  m from the guide entrance as a function of time  $t$  elapsed after the launch of a single atom packet, at the velocity  $v_i = 80$  cm/s (with a rms velocity dispersion of 20 cm/s). (a): The IP traps have a depth of 50 G and a minimum field of 1 G, and one varies  $v_{\text{conv}}$ . A sharp peak of trapped atoms arrives at a time  $t_p$ . When the velocity mismatch between the conveyor and the injected atoms is too large, extra peaks corresponding to untrapped atoms appear (\*). (b): Arrival time  $t_p$  of the trapped atoms (squares) as a function of  $v_{\text{conv}}$ ;  $t_p$  is essentially equal to  $z_2/v_{\text{conv}}$  (dashed line). (c): The conveyor speed is fixed at 50 cm/s and one varies the IP trap depth. For too shallow traps, one gets a peak of untrapped atoms (\*); if the depth is too high, some atoms are reflected, which decreases the peak amplitude.

during the motion. The MOT region is protected by a magnetic shield from the influence of the conveyor and solenoid fields (see Fig. 2).

We first investigate the transport of a single atom cloud launched into the potential resulting from the guide and the conveyor. With a resonant probe located at  $z_2 = 1.7$  m from the guide entrance, we measure the time-dependant atomic density  $n(z_2, t)$ . Figure 3a shows the corresponding signals for a chain of IP traps with a 50 G depth and a minimum of 1 G. The velocity of the packet before entering the conveyor is  $v_i = 80$  cm/s, with a rms dispersion of 20 cm/s, and we study different conveyor velocities  $v_{\text{conv}}$ . Without conveyor (bottom curve), the temporal width of the signal exceeds one second, due to the large spreading of the packet during its free flight. When the conveyor is running at a velocity around  $v_i$ , one gets a sharp peak arriving at the time  $t_p \sim z_2/v_{\text{conv}}$  (Fig. 3b) corresponding to atoms that have been trapped in the conveyor. Indeed, for those atoms, the spreading is frozen out during the transport, thus avoiding a decrease in the atomic density. The width of the absorption signal is set by the residual spreading over 30 cm once the atoms are released from the conveyor.

A significant fraction of the atoms are captured even if  $v_{\text{conv}}$  differs significantly from  $v_i$  (see, *e.g.*, the curve

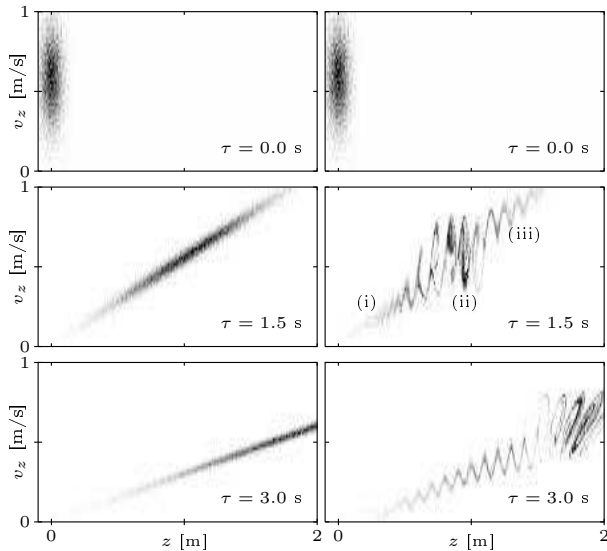


FIG. 4: Simulated atomic distribution in phase-space ( $z, v_z$ ) for various times  $\tau$  after the launch of the packet. The initial velocity is  $v_i = 60$  cm/s, with a 20 cm/s dispersion, and the initial size of the packet is 5 cm. Left: free propagation (no conveyor), showing the spatial spreading of the packet and the building of correlations between position and velocity. Right: the conveyor is made of IP traps with 10 G height, moving at  $v_{\text{conv}} = 60$  cm/s. At  $\tau = 1.5$  s, the slow (i), trapped (ii) and fast (iii) atoms are easily identified. At  $\tau = 3$  s, the atom packets released from the conveyor have already started to spread out and overlap.

for  $v_{\text{conv}} = 50$  cm/s). For a large velocity mismatch, one observes a class of atoms that are not trapped. If  $v_i > v_{\text{conv}}$ , these untrapped atoms are too energetic to be trapped, ‘fly’ over the longitudinal barriers, and arrive at the probe location before the trapped ones. Conversely, if  $v_i < v_{\text{conv}}$ , one observes a peak arriving at large times, corresponding to slow atoms. The best capture efficiency is obtained for  $v_{\text{conv}} \simeq v_i$ . The lowest transport velocity we have been able to achieve is as low as  $v_{\text{conv}} = 25$  cm/s, for which collisions with the background gas start to decrease significantly the number of trapped atoms reaching the probe region.

We then study the influence of the depth of the conveyor potential on the capture. Figure 3c depicts the signal obtained when launching atoms at  $v_i = 80$  cm/s into a conveyor running at  $v_{\text{conv}} = 50$  cm/s, for various depth of the IP wells: 22, 42 and 64 G. If the barrier heights are too low, one clearly distinguishes a peak corresponding to fast, untrapped atoms. When raising the barrier heights, this peak disappears. If the barriers are too high, the overall signal starts to decrease as many atoms are reflected at the conveyor entrance.

For a better understanding of the trapping process, we have developed a numerical simulation of the atomic trajectories in the conveyor belt potential. It gives results in very good agreement with the observed arrival

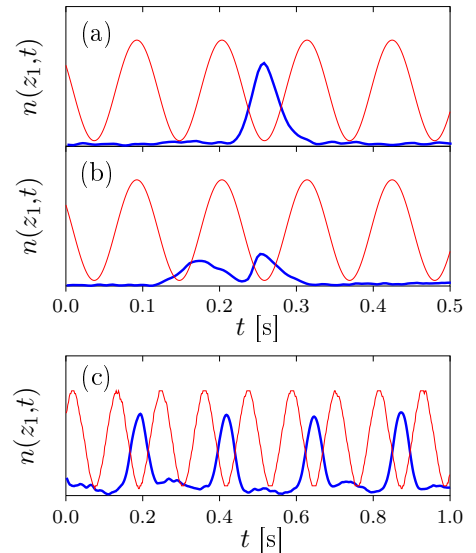


FIG. 5: (Color online). Absorption signal (thick line) measured *in the conveyor belt*, with a probe located at  $z_1 = 1$  m. The IP traps have a depth of 32 G, and one has  $v_{\text{conv}} = v_i = 88$  cm/s. The thin line is the measured  $B_z$  field component produced by the conveyor. (a): Proper synchronization of the launching of one packet to load a single trap (the cloud arrives in coincidence with a potential minimum). (b): The launching occurs at a time  $\Lambda/(2v_{\text{conv}})$  before, resulting in a splitting of the cloud into two consecutive traps. (c): Multiple injection of packets, with the proper synchronization to load one every second trap.

time signals and confirm that, depending on the barrier height and on the velocity mismatch between the conveyor and the injected packets, atoms can: (i) be considerably slowed down during the entrance (low  $v_i$ , large height), some of them being even reflected; (ii) be trapped in the conveyor wells; and (iii) be too energetic to be trapped and simply pass over the conveyor barriers (large  $v_i$ , low height). Figure 4 presents plots of the atomic distribution in the phase-space ( $z, v_z$ ), at a time  $\tau$  after the launch of the packet, obtained by numerical simulation. These plots allow for an easy identification of the various classes of atoms. The slowing of the atoms of class (i) by the time-dependent potential is reminiscent of the Stark deceleration technique used for beams of polar molecules [12], and can be understood qualitatively as the result of a reflection of the atoms on a moving potential wall [13]. It is clear from such plots that the spatial spreading of the trapped clouds is frozen during the transport. Here, the initial size and velocity spread of the packet are such that several conveyor wells are loaded.

For an optimal loading of a single trap, three conditions need to be fulfilled. First, our simulations confirm that, as one expects intuitively, the energy of the trapped atoms in the conveyor frame is minimum when the velocities are matched  $v_i \simeq v_{\text{conv}}$ . Second, the length of the

packet at the entrance of the conveyor has to be smaller than the distance between adjacent traps. Finally, a careful synchronization of the launching with respect to the conveyor motion is required. This is essential to avoid a splitting of the cloud between two adjacent wells (see Fig. 5a and b). When those conditions are fulfilled, typically  $N \sim 10^9$  atoms are trapped, which corresponds, according to our simulations, to 75% of the incoming packet.

We now turn to the injection of multiple packets into the conveyor belt. In order to demonstrate the trapping efficiency of the conveyor, we use the probe at  $z_1 = 1$  m (*i.e.*, inside the conveyor zone) and inject atoms with the proper synchronization in order to capture one cloud every second IP trap (Fig. 5c). When released from the conveyor, those packets spread out and overlap, yielding a continuous beam. We investigated the effect of the conveyor on the beam's temperature, and find no detectable heating within our experimental accuracy: for  $v_{\text{conv}} = v_i = 1$  m/s, one has  $T = 600 \pm 20$   $\mu\text{K}$  without conveyor, and  $590 \pm 20$   $\mu\text{K}$  with a conveyor having a 35 G height. This result is compatible with our numerical simulations: for our parameters, the heating ( $\sim 10$   $\mu\text{K}$ ) associated with the presence of the conveyor is negligible with respect to the initial temperature. The proper synchronization of the injection of packets is limited in our current setup to velocities above  $\sim 80$  cm/s. For lower velocities, the longitudinal size of the packet at the conveyor entrance already exceeds the distance  $\Lambda$  between adjacent IP traps, due to the non-adiabaticity of the entrance into the guide, and to the transverse compression of the confining potential over the first 40 cm of the guide (see Fig. 2).

This chain of IP traps constitutes a very simple way of transporting and cooling in parallel many atomic clouds. The next step is to combine this transport with evaporative cooling, thus paving the way for the parallel production of Bose-Einstein condensates as well as for the achievement of a cw atom laser. For our parameters, the collision rate within one trapped packet is already on the order of  $10$  s $^{-1}$ , which has allowed for a first demonstration of evaporation. Using radio-frequency fields, we have been able to remove selectively the untrapped atoms and, moreover, to decrease the beam's temperature by a factor of two, reaching  $280 \pm 10$   $\mu\text{K}$ , with a flux reduction by a factor of four. Those preliminary results are encouraging in view of the realization of a new experimental set-up, designed on purpose for the use of such a scheme.

In view of the achievement of a cw atom laser through direct evaporation of an atomic beam [3], the use of a train of IP traps combined with evaporation would allow for the realization of an ultra-slow, but still supersonic, atomic beam (the latter condition being essential in order

not to decrease drastically the atomic flux [14]). For that purpose, one would capture packets of atoms at low speed into the conveyor, and then compress them adiabatically by increasing the strength of the transverse confinement. The resulting hot and dense clouds can then be evaporatively cooled. An interesting strategy consists in reaching a temperature  $T$  that satisfies  $k_B T \ll mv_{\text{conv}}^2$ , so that the packets can be released into the guide to overlap and form a very slow continuous supersonic beam. Compared to the direct injection of packets into the guide, (i) the effect of the initial longitudinal dilution due to the spreading of packets is minimized, (ii) the efficiency of the 3D evaporation is higher than its 2D counterpart [15], and (iii) the time available for evaporation is increased considerably, as the beam's velocity is set by  $v_{\text{conv}}$ , which can be as low as 10 cm/s. The corresponding final temperature then needs to be smaller than 10  $\mu\text{K}$ . One could apply, on the atomic beam obtained this way, the final evaporation stages in order to achieve quantum degeneracy.

We thank Jean Dalibard for a careful reading of the manuscript, and the ENS laser cooling group for fruitful discussions. We acknowledge financial support from the Délégation Générale pour l'Armement (DGA) and Institut Francilien de Recherche sur les Atomes Froids (IFRAF). Z. W. acknowledges support from the European Marie Curie Grant MIF1-CT-2004-509423, and G. R. support from the DGA.

- 
- [\*] Unité de Recherche de l'École Normale Supérieure et de l'Université Pierre et Marie Curie, associée au CNRS.
  - [1] E. A. Cornell and C. E. Wieman, *Rev. Mod. Phys.* **74**, 875 (2002); W. Ketterle, *ibid.*, **74**, 1131 (2002).
  - [2] K. Helmerson, D. Hutchinson, and W. Phillips, *Physics World* **12**, 31 (1999) and refs. therein.
  - [3] E. Mandonnet *et al.*, *Eur. Phys. J. D* **10**, 9 (2000).
  - [4] T. Lahaye *et al.*, *Phys. Rev. A* **72**, 033411 (2005).
  - [5] H. J. Lewandowski *et al.*, *J. Low Temp. Phys.* **132**, 309 (2003).
  - [6] M. Greiner *et al.*, *Phys. Rev. A* **63**, 031401 (2001).
  - [7] W. Hänsel *et al.*, *Phys. Rev. Lett.* **86**, 608 (2001).
  - [8] P. Hommelhoff *et al.*, *New J. Phys.* **7**, 3 (2005).
  - [9] T. Lahaye *et al.*, *Phys. Rev. Lett.* **93**, 093003 (2004).
  - [10] E. A. Hinds and I. G. Hughes, *J. Phys. D: Appl. Phys.* **32**, R119 (1999).
  - [11] J. J. Tollet *et al.*, *Phys. Rev. A* **51**, R22 (1995).
  - [12] H. L. Bethlem, G. Berden, and G. Meijer, *Phys. Rev. Lett.* **83**, 1558 (1999).
  - [13] A. Steyerl, *Nucl. Instrum. Methods* **125**, 461 (1975).
  - [14] J. M. Vogels *et al.*, *J. Phys. IV France* **116**, 259 (2004).
  - [15] W. Ketterle and N. J. Van Druten, *Adv. At. Mol. Opt. Phys.* **37**, 181, (1996).